ARTICLE OPEN

Microglial PCGF1 alleviates neuroinflammation associated depressive behavior in adolescent mice

Naigang Li[1], Jingyi Du[1], Ying Yang[2], Tiantian Zhao[1], Dong Wu[1], Fan Peng[1], Dongshuang Wang[1], Linghua Kong[3]✉, Wenjuan Zhou[1]✉ and Aijun Hao[1]✉

© The Author(s) 2024

Epigenetics plays a crucial role in regulating gene expression during adolescent brain maturation. In adolescents with depression, microglia-mediated chronic neuroinflammation may contribute to the activation of cellular signaling cascades and cause central synapse loss. However, the exact mechanisms underlying the epigenetic regulation of neuroinflammation leading to adolescent depression remain unclear. In this study, we found that the expression of polycomb group 1 (PCGF1), an important epigenetic regulator, was decreased both in the plasma of adolescent major depressive disorder (MDD) patients and in the microglia of adolescent mice in a mouse model of depression. We demonstrated that PCGF1 alleviates neuroinflammation mediated by microglia in vivo and in vitro, reducing neuronal damage and improving depression-like behavior in adolescent mice. Mechanistically, PCGF1 inhibits the transcription of MMP10 by upregulating RING1B/H2AK119ub and EZH2/H3K27me3 in the MMP10 promoter region, specifically inhibiting microglia-mediated neuroinflammation. These results provide valuable insights into the pathogenesis of adolescent depression, highlighting potential links between histone modifications, neuroinflammation and nerve damage.

Molecular Psychiatry (2025) 30:914–926; https://doi.org/10.1038/s41380-024-02714-2

INTRODUCTION

Depression is a common psychiatric disease worldwide [1, 2] that affects approximately one in five people at some point in their lives [3]. Adolescent depression is more worrisome due to its occurrence during a period of rapid physical, emotional, and cognitive development [4, 5], with adolescent depression increasing at a greater rate than in adults [6]. Notably, epigenetics and changes in brain genetics are active during adolescence [7, 8]. Transcriptome analyses have shown that brain development from the late fetal stage to adolescence is accompanied by epigenomic reorganization [9]. Epigenetics exerts crucial effects on brain function and increases the risk of neuropsychiatric disorders [10–12]. Thus, epigenetics is associated to the development of mental illnesses in adolescence.

Epigenetics may provide new insights into the long-term effects of gene expression regulation associated with depression [13]. Epigenetics refers to the modification of gene expression by regulating the transcription, posttranscription, translation or posttranslation of the genome, such as through DNA methylation, DNA hydroxymethylation, and histone modifications [14, 15]. These epigenetic effects have been widely investigated in various psychiatric conditions [16–18]. Among them, histone modifications are major epigenetic mechanisms [19]. Histone modifications alter the chromatin structure by affecting histone-DNA and histone-histone interactions, thus regulating gene transcription [20, 21]. The main histone modifications include acetylation, phosphorylation, methylation, and ubiquitination [22]. Numerous studies have indicated that histone modifications are actively involved in the regulation of neuroinflammation [23–25] and play a role in the onset and development of psychiatric disorders, including autism spectrum disorder (ASD), schizophrenia and major depressive disorder (MDD) [26–29].

Polycomb group factor 1 (PCGF1), also known as Nspc1, is an essential epigenetic regulator that belongs to the polycomb group (PcG) of proteins [30]. The PcG proteins include polycomb repressor complexes 1 and 2 (PRC1 and PRC2), which repress gene expression by recognizing the CpG islands (CGIs) of target genes [31, 32]. PRC1 mediates the monoubiquitination of lysine 119 of histone H2A (H2AK119ub1) via the E3 ubiquitin ligases RING1A and RING1B. PRC2 mediates trimethylation of lysine 27 of histone H3 (H3K27me3) via the histone methyltransferase EZH1/2 [33–35]. PCGF1 forms the core of the noncanonical PRC1.1 complex (nc-PRC1.1) with RING1A or B, KDM2B (lysine demethylase 2B), and BCOR (BCL6 corepressor) [36]. Deletion of PCGF1 has the greatest impact on H2AK119ub1 deposition by PRC1 [34], while PRC1.1-mediated deposition of H2AK119ub1 promotes the recruitment of PRC2, which in turn promotes the deposition of H3K27me3 [31, 36, 37]. Therefore, PCGF1 plays a vital role in the PCGF family. Current research on PCGF1 has focused mainly on embryonic development [38–40], tumor stem cell self-renewal [30, 41, 42], and hematopoietic stem cell differentiation [43, 44], while its function in neuroinflammation and adolescent depression is still unknown.

[1]Key Laboratory for Experimental Teratology of Ministry of Education, Shandong Key Laboratory of Mental Disorders, Department of Anatomy and Histoembryology, School of Basic Medical Sciences, Cheeloo College of Medicine, Shandong University, Jinan, China. [2]Childhood Psychiatry Unit, Shandong Mental Health Center, Jinan, China. [3]School of Nursing and Rehabilitation, Cheeloo College of Medicine, Shandong University, Jinan, China. ✉email: konglinghua@sdu.edu.cn; wenjuanzhou@sdu.edu.cn; aijunhao@sdu.edu.cn

Received: 27 September 2023 Revised: 15 August 2024 Accepted: 22 August 2024
Published online: 30 August 2024

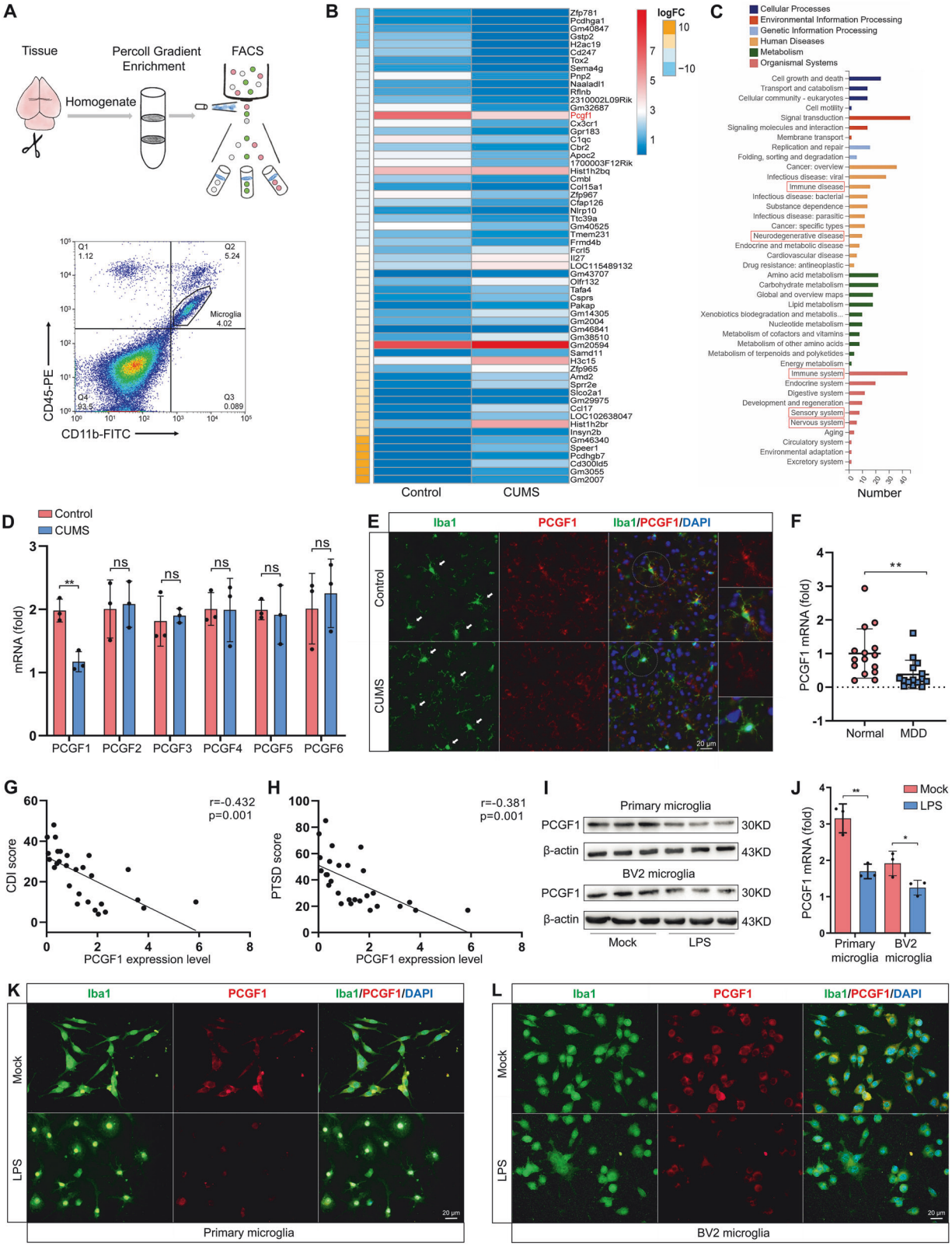

Microglia are resident immune cells in the central nervous system (CNS). These cells can be rapidly activated depending upon distinct stimulatory contexts, resulting in neuroinflammation [45, 46]. Moreover, brain autopsies of depressed patients have confirmed the activation of microglia and neuroinflammation [47]. Neuroinflammation is believed to contribute to decreased neurotrophic support, altered glutamate release/reuptake, and oxidative stress, ultimately leading to excitotoxicity and neuronal injury [48, 49]. Neuroinflammation is also one of the main hypotheses of depression.

Fig. 1 PCGF1 was downregulated in microglia of CUMS mice and the plasma of MDD adolescent patients. A Experimental protocol for FACS and gate strategy for CD11b^{+}CD45Low microglia was presented. **B** Heat map of 30 up- and downregulated expression of genes in microglia. **C** KEGG analysis revealed that the differentially expressed genes were enriched in immune and neurological diseases. **D** QPCR analysis of PCGF1-6 mRNA levels in microglia ($N = 3$ per group). **E** Representative images of PCGF1 staining (red) in the CUMS mice. Nuclei (blue) are stained with DAPI. Microglia (green) are stained with Anti-Iba1. Scale bar is 20 μm. **F** Levels of PCGF1 were decreased in the plasma of MDD adolescent patients ($n = 15$) compared with those of normal controls (n = 15). **G**, **H** Correlation between PCGF1 expression and CDI or PTSD scores using the Pearson's correlation coefficient ($n = 28$). **I** Representative western blot images showing the expression levels of PCGF1 ($N = 3$ per group). The mock treatment was a blank control with the addition of PBS (dissolvent for LPS). **J** QPCR analysis of PCGF1 mRNA levels ($N = 3$ per group). **K**, **L** Representative images of PCGF1 staining (red) in the LPS stimulated primary and BV2 microglia. Nuclei (blue) are stained with DAPI. Microglia (green) are stained with Anti-Iba1. Scale bar is 20 μm. Statistical significance was determined by multiple unpaired two-sided Student's *t*-tests or one-way ANOVA followed by Tukey post hoc test. Data are shown as the mean±s.d. or as a representative result from three independent experiments. $^{*}P < 0.05$, $^{**}P < 0.01$ and $^{***}P < 0.001$.

In the present study, we investigated the potential mechanisms of stress-induced neuroinflammation in the pathogenesis of depression. Many brain regions have been implicated in depression, such as the prefrontal cortex, amygdala and hippocampus [50, 51]. Hippocampal dysfunction is a key factor in the neuropathology of MDD, particularly the cornu ammonis 1 (CA1) region is an important brain region that is prone to synaptic plasticity. An increasing number of studies have shown that the CA1 region is involved in the pathogenesis of depression to regulate mood and cognitive function [52, 53]. It has also been demonstrated that in patients with MDD, the left CA1 is the hippocampal subregion most strongly associated with childhood abuse [54]. We found that PCGF1 in microglia of the CA1 region plays a key role in maintaining immune homeostasis at this site, which protects the structure and function of neurons associated with depression. These results suggest previously unexplored avenues of research to develop potential therapeutic targets for the treatment of this disorder.

MATERIALS AND METHODS

Animals and housing conditions

Male C57BL/6J mice weighing 12–14 g (about 3 weeks) were purchased from the Experimental Animal Centre of Shandong University. Mice were housed under a 12 h light/dark cycle and had free access to food and water. Ambient temperature was maintained at 22 °C ± 2 °C, except when subjected to the conditions of specific experiments. All efforts were made to minimize the pain and numbers of the animals used in the experiments. All animal care and experiments followed the National Institutes of Health Guide for the Care and Use of Laboratory Animals and were approved by the Institutional Animal Care and Use Committee of Shandong University.

Study approval and subjects

The Ethics Committee of Shandong Mental Health Center (Jinan, 250014, China) approved all materials and procedures. The clinical trial registration number is (2021) ethical review No. (99). All participants or their legally authorized representatives provided written informed consent to participate in this study. Adolescent patients with MDD were recruited through inpatients of the Department of Shandong Mental Health Center. Healthy control subjects were recruited through local community postings and media advertisements. Inclusion and exclusion criteria and behavioral measures are described in the Supplementary Information. All clinical samples were collected and experimented in accordance with WS/T 661-2020 Guidelines of venous blood specimen collection of the China Healthcare Commission and approved by the Ethics Committee of Shandong Mental Health Center.

CUMS model

Mice in the chronic unpredictable mild stress (CUMS) group were subjected to procedures described previously. Briefly, mice were assigned into control and CUMS groups by principles of random allocation. Mice in CUMS group were individually housed and subjected to a daily stress regime for five days a week and last four weeks. Stress consists of: (1) 24 h of water and food deprivation, (2) standing on ice and water mixture for 2 min, (3) damp sawdust for 24 h, (4) tail clamp for 3 min, (5) cage tilted 45°for 12 h, (6) restricted movement for 2 h and (7) horizontal oscillation for 5 min. One stressor was applied per day in a random order. Mice in the control group were housed under laboratory conditions. Behavioral tests are detailed with Supplementary Materials.

Chromatin immunoprecipitation

BV2 microglia were infected with LPS for 8 h. Formaldehyde (37%) was added directly to the culture medium to a final concentration of 1%, and cells were incubated for 10 min at 37 °C. Glycine was added to a final concentration of 125 mM to quench cross-linking. A ChIP Assay Kit (Cell Signaling Technology) was used following the manufacturer's instructions. Extracted DNA fragments were used for ChIP-QPCR and ChIP-Sequencing. Specific primers for the MMPs genome are listed in Supplementary Table 1.

RNA sequencing and ChIP-sequencing

To perform RNA sequencing (RNA-seq), microglia were harvested and lysed by TRIzol, and total RNA was collected according to the manufacturer's instructions. RNA-seq was carried out on a BGISEQ-500 (Beijing Genomic Institution, www.genomics.org.cn, BGI). The significance of the differential expression of genes was confirmed by the bioinformatics service of BGI. ChIP-Seq was carried out on a DNBSEQ (Beijing Genomic Institution, www.genomics.org.cn, BGI). Peak detection was analyzed using IGV (Integrative Genomics Viewer). Motif analysis in peaking sequences was performed using MEME Suite.

Isolation of primary microglia and LPS stimulation

Primary astrocytes and microglia were isolated from the cerebral cortex and corpus callosum of stress-naïve mice (3 days old) for subsequent in vitro experiments. These glial cells were placed in 75 cm^2 flasks (Beaver) and cultured in Dulbecco's Modified Eagle's Medium-High Glucose Medium (Gibco, United States; #11965092) containing 10% fetal bovine serum (Gibco, United States; #10099141C) and Penicillin-Streptomycin-Amphotericin Cocktail (Macgene, Beijing, China; #CC033) in culture. The flasks were then placed in a 37 °C, 5% CO2 incubator. The medium was changed every 3 days. After ~10–12 days, the mixed primary glial cells were shaken at 200 rpm and 37 °C for 4 h to harvest primary microglia. Primary microglia and BV2 microglia were stimulated with LPS (L2630, Sigma-Aldrich) 500 ng/ml for 8 h. BV2 microglia purchased from Chinese Academy of Sciences (CAS) Cell Bank were recently authenticated and tested for mycoplasma contamination.

Flow cytometry sorting of microglia

Place mice cerebral cortex ($n = 3$/group) tissue in pre-cooled Hank's Balanced Salt Solution. The tissue was cut into ~1 mm pieces, ground, and a cell suspension was produced. The cell suspension was filtered through a 70-μm sieve (431751, Corning), centrifuged at 420 × *g* for 10 min, and the precipitate was resuspended with 4 mL of 30% Percoll solution (GE17-5445-01, Sigma-Aldrich). Then, 4 mL of 70% Percoll solution was slowly added to the lower cell suspension using a syringe and centrifuged at 500 × *g* for 20 min. (One part of 10× HBSS was mixed with 9 parts of Percoll stock solution to prepare an isotonic suspension of Percoll, which we defined as a 100% suspension of Percoll. 100% Percoll was diluted with 1× PBS to produce the expected density of Percoll isolation solution for cell separation.) Cells were harvested from the layered interface of different concentrations of Percoll solution and washed once with PBS containing 0.2% BSA. Cells were stained with antibodies, FITC anti-mouse CD11b (M1/70, Biolegend) or APC anti-mouse CD45 (QA17A26, Biolegend), and CD45-low/CD11b+ microglial cells were sorted using a flow cytometer Moflo Astrios EQ.

Inclusion and exclusion criteria

For individuals in the MDD adolescent patients group, subjects were required to meet the following criteria: (1) Meet the diagnostic criteria for

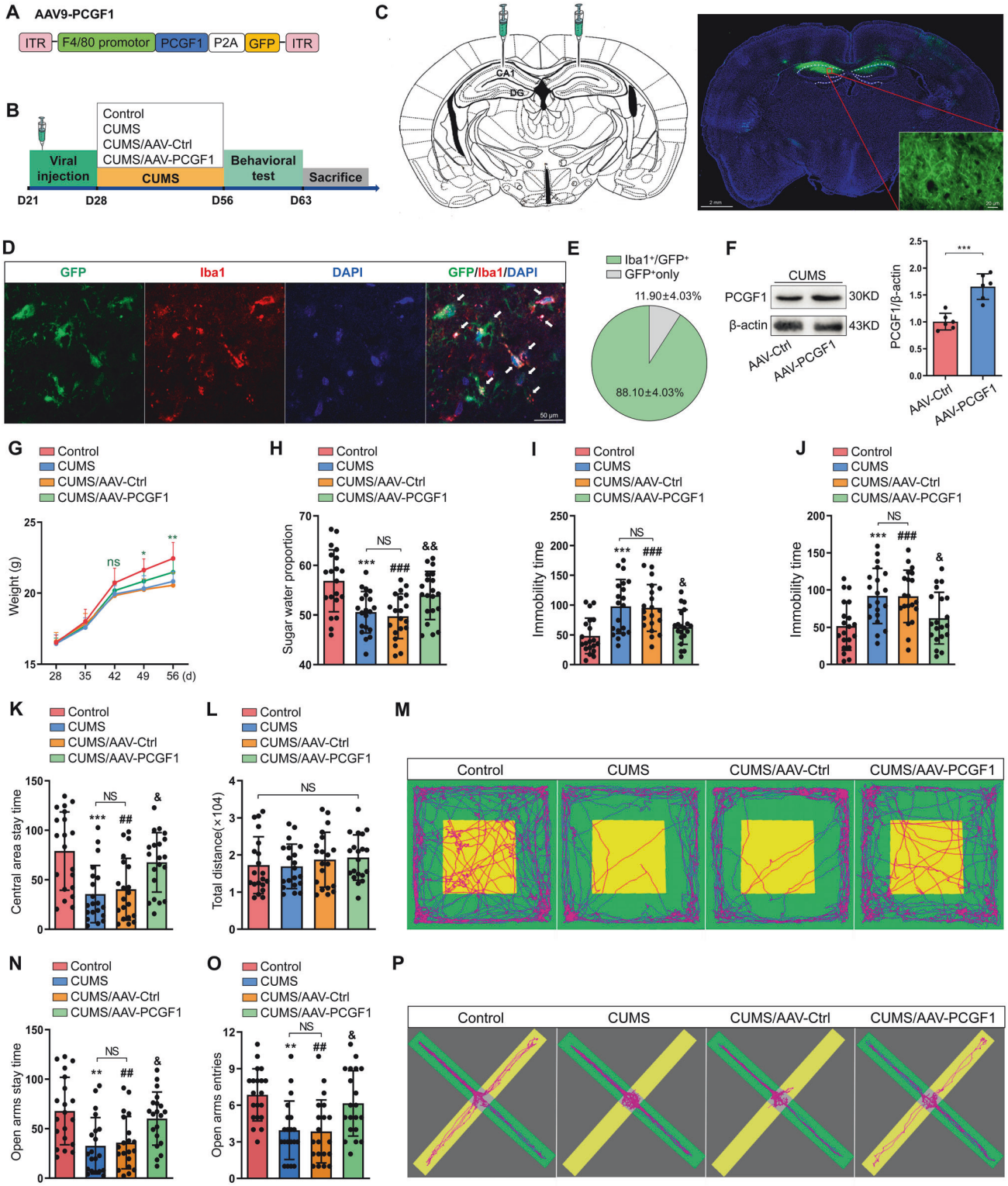

MDD using a Structured Clinical Interview by two neuropsychiatrists according to the Diagnostic Statistical Manual of Mental Disorder, Fifth Edition (DSM-V); (2) The scores is larger than 19 which was measured by the children's depression inventory (CDI); (3) Drug naïve or drug free for longer than three weeks (includes antidepressants and dependence-producing drugs such as narcotics), and no history of substance abuse; (4) Aged between 10 and 20. Exclusion criteria for healthy controls included history of neuropsychiatric disorders, head injury, substance abuse (includes antidepressants and dependence-producing drugs such as narcotics), or unconsciousness. (Additional clinical and scale-related information references supplementary materials and methods.)

Statistical analyses

All data were collected and processed randomly or in a counterbalanced manner. Experimenters were unaware of the treatments and data analyses were performed blindly. The figure legend lists the number of subjects and biological replicates independently processed in each experimental

Fig. 2 Microglial PCGF1 is associated with depression-like behavior in CUMS mice. A Schematics of AAV vectors engineered to overexpress PCGF1. **B** Experimental paradigm for determining behavioral responses of mice infected with the virus. **C** Schematics of AAV vectors and bilateral injection sites in the CA1 region of hippocampus. Scale bar, 2 mm and 20 μm. GFP, Green fluorescent protein. CA, Cornu Ammonis. DG, dentate gyrus. **D** Colocalization of GFP (green) and Iba1 (red), scale bar, 50 μm. **E** Iba1$^+$/GFP$^+$ percentage statistics. **F** Representative western blot images of PCGF1 in the CA1 region and analysis of expression efficiency ($N = 6$ per group). **G** Microglial PCGF1 reverses weight loss in CUMS mice ($N = 20$ per group). **H** Microglial PCGF1 reverses the reduction of sucrose solution consumption in CUMS mice ($N = 20$ per group, * CUMS vs. Control; # CUMS/AAV-Ctrl vs. Control; & CUMS/AAV-PCGF1 vs. CUMS/AAV-Ctrl, same as below). **I, J** In CUMS mice, microglial PCGF1 reverses the increased immobility time in FST and TST ($N = 20$ per group). **K** In CUMS mice, microglial PCGF1 increases the stay time in the central area during the OFT test ($N = 20$ per group). **L** Total distance traveled in the OFT was not significantly different ($N = 20$ per group). **M** Representative activity tracking in the OFT. **N, O** In CUMS mice, microglial PCGF1 increases the stay time and the number of entries in the open arms during the EPM test ($N = 20$ per group). **P** Representative activity tracking in the EMP. Statistical significance was determined by multiple unpaired two-sided Student's *t*-tests or one-way ANOVA followed by Tukey post hoc test. Data are shown as the mean±s.d. or as a representative result from three independent experiments. *$P < 0.05$, **$P < 0.01$ and ***$P < 0.001$. # and & follows the same rules.

condition. Statistical methods were not used to predetermine sample sizes, but our sample sizes were similar to those reported in previous publications.

Statistical analyses were conducted using GraphPad Prism version 8 (GraphPad Software, Inc.). We tested the normality of the data using the Shapiro–Wilk test. Comparisons between two groups were performed using a two-tailed Student's *t*-test. Comparisons among multiple groups were conducted using a one-way ANOVA followed by Tukey post hoc test. The data are presented as the mean ± SD. A statistically significant difference was defined as $P < 0.05$.

RESULTS

Neuroinflammation is induced in specific brain regions of CUMS mice

We first evaluated the behavior of mice subjected to chronic unpredictable mild stress (CUMS), as assessed by the forced swimming test (FST) and sucrose preference test (SPT) (Fig. S1A). The immobility times of CUMS mice in the FST were significantly increased and the percent of sucrose consumption of CUMS mice in the SPT was also significantly reduced (Fig. S1B, C). These results suggest that the CUMS protocol is effective in inducing depression-like behavior. Quantitative polymerase chain reaction (QPCR) assay revealed increased expression of Interleukin-1β (IL-1β, Fig. S1D), Interleukin-6 (IL-6, Fig. S1E) and Tumor necrosis factor α (Tnf-α, Fig. S1F) in the hippocampus, ventromedial prefrontal cortex (vmPFC) and cortex regions in CUMS mice. The hippocampus is an important brain region involved in the pathogenesis of depression [55], so we further performed immunofluorescence assay of the hippocampus. The results of the immunofluorescence assay showed higher levels of Iba1 (Fig. S1G), IL-1β (Fig. S1H), and Tnf-α (Fig. S1I) in the hippocampus of CUMS mice (Fig. S1J), especially in the CA1 region.

PCGF1 is downregulated in microglia of CUMS mice and the plasma of MDD adolescent patients

In order to accurately investigate microglia in the brain of CUMS mice, we sorted out CD11b$^+$CD45^{low} microglia from whole brain (Fig. 1A) and performed RNA sequencing. RNA sequencing analysis revealed that the expression of 214 genes were downregulated and 50 genes was upregulated in CUMS mice, log2(Fold Change) > 1 and *Q*-value < 0.05 (Fig. S2A). As shown in Fig. 1B, the heat map generated showed top 30 up- and downregulated expression of genes. Next, Kyoto Encyclopedia of Genes (KEGG) analysis observed these differentially expressed genes were enriched in immune responses and neurological diseases (Fig. 1C). KEGG analysis also revealed that these genes were mainly involved in inflammatory signaling pathways, such as NF-κB and Tnf-α signaling pathways (Fig. S2B). In the RNA sequencing results, we found a significant downregulation of the important epigenetic regulator PCGF1, with log2(Fold Change) = –2.81 and *Q*-value < 0.05 (Fig. 1B). However, the function of PCGF1 in microglia is still unknown, which aroused our research interest. Subsequently, we analyzed the expression of 1-6 members of the PCGF family in microglia of CUMS mice. As shown, only the expression of PCGF1 was significantly downregulated (Fig. 1D). Immunofluorescence results similarly showed that microglial PCGF1 expression was downregulated in CUMS mice (Fig. 1E, S2E), while PCGF1 expression was unchanged in neurons (Fig. S2C, S2E). Also, we found that PCGF1 was very poorly expressed in astrocytes (Fig. S2D). These results imply that microglial PCGF1 in CUMS mice may have cell-specific functions. To determine whether PCGF1 is associated with adolescent depression, we examined plasma levels of PCGF1 in normal controls and MDD adolescent patients. The sociodemographic and clinical characteristics of these subjects are shown in Supplementary Table 2. As shown in Fig. S2F, G, we recorded the subjects' scores on the children's depression inventory (CDI) and post-traumatic stress disorder (PTSD) scales. QPCR results showed that PCGF1 mRNA levels were significantly lower in MDD adolescent patients compared to normal controls (Fig. 1F). In addition, we observed a negative correlation between PCGF1 levels and CDI, PTSD scores (Fig. 1G, H). In vitro experiments, we used lipopolysaccharide (LPS) to stimulate primary and BV2 microglia-mediated inflammation to mimic the neuroinflammation caused by CUMS in vivo. We found that LPS stimulation significantly reduced the protein and mRNA level of PCGF1 in microglia (Figs. 1I, J, and S2H). Immunofluorescence assay also suggest the same results (Figs. 1K, L, S2I).

Microglial PCGF1 in the CA1 region is associated with depression-like behavior in CUMS mice

To ascertain whether PCGF1 was related to depression-like behavior, we specifically induced PCGF1 overexpression in microglia by directly injecting microglia-specific AAV9-F40/80-PCGF1-GFP virus into the hippocampus CA1 region of the CUMS mice (Fig. 2A, B). Successful virus targeting was indicated by the observation of large amounts of green fluorescence (GFP) within the CA1 region at five weeks post-injection (Fig. 2C). While GFP expression was particularly concentrated on Iba1 cells (Fig. 2D, E) and little expression on neurons and astrocytes (Fig. S3A, S3B). Furthermore, we confirmed successful overexpression of PCGF1 in the CA1 region via western blotting (Fig. 2F). CUMS mice exhibited decreased body weight (Fig. 2G), reduced sucrose solution consumption (Fig. 2H) and increased immobility time in FST (Fig. 2I) and Tail suspension test (TST, Fig. 2J), all of which are indicative of depression-like behavior. However, these behaviors were reversed following upregulation of PCGF1 in microglia. In the open field test (OFT), CUMS exposure did not affect the total distance traveled by the mice (Fig. 2L) but decreased the duration and frequency of mice exploring the central area (Figs. 2K, M, and S3C). Furthermore, the results of the elevated maze (EPM) test showed that CUMS exposure reduced the duration and frequency of mice entering the open arm (Fig. 2N–P). Nonetheless, upregulation of PCGF1 reversed the anxiety-like behavior of CUMS mice in both OFT and EMP. Taken together, overexpression of microglial PCGF1 ameliorates CUMS-induced depression-like behavior in mice.

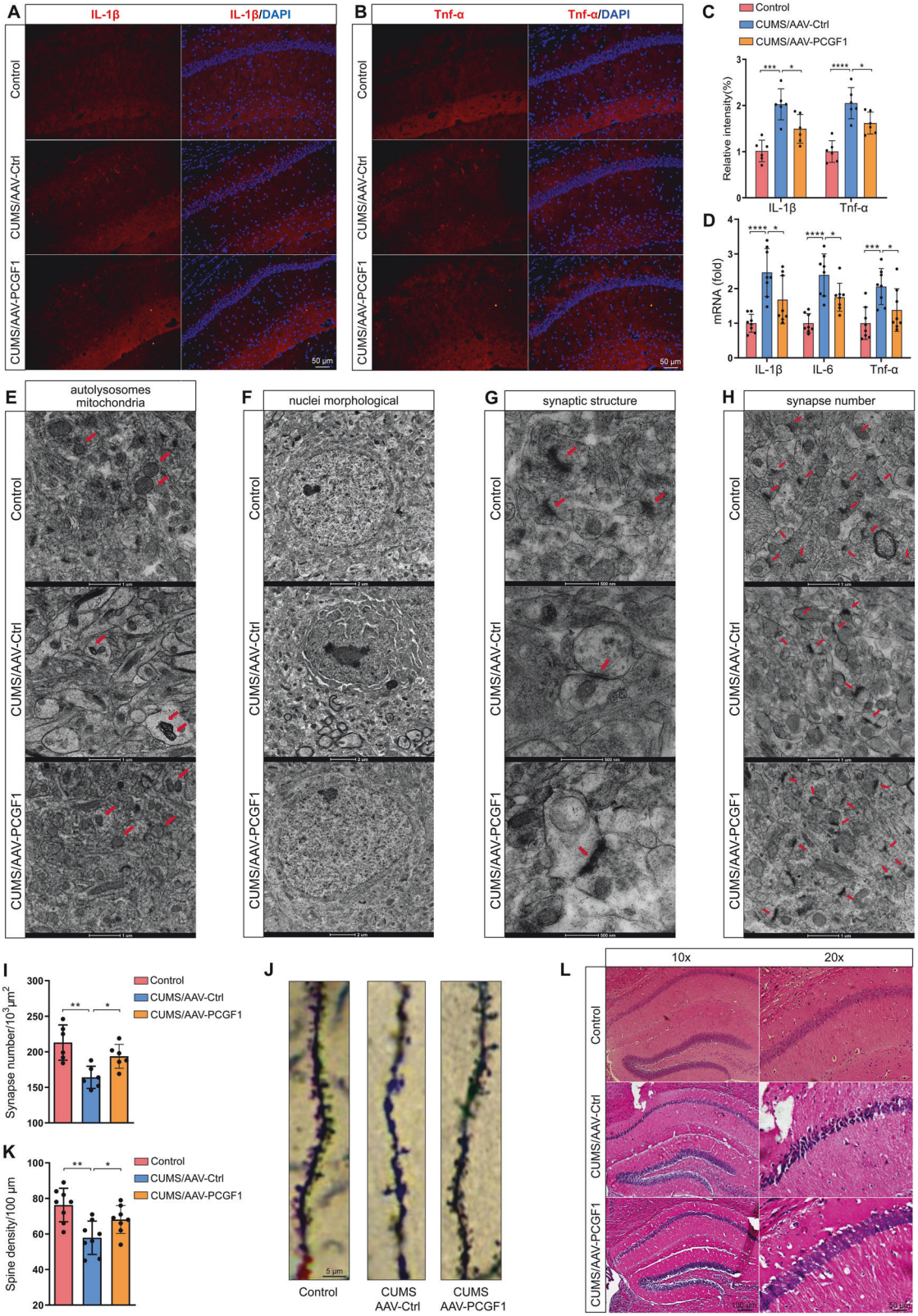

PCGF1 regulates neuroinflammation and neuronal damage in the CA1 region of CUMS mice

Next, by immunofluorescence assay, we were able to observe that overexpression of microglia PCGF1 reversed the expression of IL-1β and Tnf-α in the CA1 region of CUMS mice (Fig. 3A–C). In addition, we observed the mRNA expression of IL-1β, IL-6, and Tnf-α inflammatory factors was also reversed (Fig. 3D). These results suggested that overexpression of PCGF1 in microglia

Fig. 3 Microglial PCGF1 alleviates neuroinflammation and decreases neuronal damage. A, **B** Representative images of IL-1β and Tnf-α staining (red). Nuclei (blue) are stained with DAPI. Scale bar is 50 μm ($N = 6$ per group). **C** Fluorescence intensity analysis of A and B. **D** QPCR analysis of IL-1β, IL-6 and Tnf-α mRNA levels of CA1 region ($N = 8$ per group). **E** Representative TEM of autolysosomes and morphology of mitochondria. Arrows indicate autolysosomes. Scale bar is 1 μm. **F** Representative TEM showing the apoptotic features in the nuclei of CA1 neurons. Scale bar is 2 μm. **G** Representative TEM of neuronal synapses. Arrows indicate neuronal synapses. Scale bar is 500 nm. **H**, **I** Representative TEM and summary of data showing the number of synapses. Arrows indicate neuronal synapses. Scale bar is 1 μm ($N = 6$ per group). **J** Representative images of dendrites in pyramidal neurons. Scale bar is 5 μm. **K** Quantification of mushroom spines in neurons. **L** Representative photomicrographs of H&E staining in CA1 region. For magnification ×10, Scale bar is 100 μm; for magnification ×20, Scale bar is 50 μm. Statistical significance was determined by multiple unpaired two-sided Student's *t*-tests or one-way ANOVA followed by Tukey post hoc test. Data are shown as the mean±s.d. or as a representative result from three independent experiments. $^{*}P < 0.05$, $^{**}P < 0.01$ and $^{***}P < 0.001$.

reduced the neuroinflammation in the CA1 region of CUMS mice. The transmission electron microscopy (TEM) revealed that microglial PCGF1 alleviated CUMS-induced degraded mitochondria and increased number of autolysosomes (Figs. 3E, S3D). Notably, TEM analysis revealed significant apoptotic features in the nuclei of neurons (including nuclear chromatin margination, aggregation and condensation) (Figs. 3F, S3E), and impaired synaptic plasticity (Fig. 3G). However, microglial PCGF1 alleviated those abnormalities. Meanwhile, microglial PCGF1 also reduced neuronal restructuring abnormalities in CUMS mice, such as reduced number of synapses (Fig. 3H, I) and reduced density of dendritic spines in Golgi-staining (Fig. 3J, K). Additionally, microglial PCGF1 ameliorated the neuronal morphological damage in the CA1 region of CUMS mice, as evidenced by H&E staining (Figs. 3L and S3F). Those findings presented evidence that microglial PCGF1 in the CA1 region reduce neuroinflammation, thereby slowing down neuronal apoptosis and structural damage, and ultimately ameliorating depression-like behavior in CUMS mice.

Microglial PCGF1 regulates LPS-induced neuroinflammation by MMPs members

Subsequently, we used plasmid and lentivirus to overexpress and knockdown PCGF1 in LPS-induced primary microglia and BV2 microglia. We examined the efficiency of overexpression and knockdown (Fig. S4A–D). We found that overexpression of PCGF1 decreased mRNA or protein levels of IL-1β, IL-6, and Tnf-α in both cells (Fig. 4A–D). The results also showed that knockdown of PCGF1 produced the opposite results (Fig. S4E–H). Thus, PCGF1 reduces the expression of inflammatory factors in microglia. In addition, we found that primary microglia activated by LPS become amoeboid morphology with an increased branches number, but PCGF1 alleviated this activation (Figs. 4E and S4I). Meanwhile, PCGF1 inhibits LPS-induced migration of BV2 cells to open areas in scratch assays (Fig. S4J, S4K).

To explore specific mechanisms by which PCGF1 regulates neuroinflammation, we performed RNA sequencing on primary microglia transfected with PCGF1 plasmid and induced by LPS. Compared with Mock, RNA-seq analysis revealed that the expression of 3357 genes was upregulated in LPS-induced primary microglia, with log2(Fold Change) > 1 and Q-value < 0.05 (Fig. S5A; Expression heat map, Fig. S5B). As shown in Fig. 4F, several matrix metalloproteinases (MMPs) members were upregulated in primary microglia after LPS induction. Interestingly, we observed that several of these MMPs members were suppressed by PCGF1 overexpression, as shown in the volcano plot of Fig. 4G. Next, we used KEGG analysis to reveal that the differentially expressed genes after PCGF1 transfection were mainly involved in inflammatory signaling pathways (Fig. 4H). KEGG analysis also observed these genes were enriched in immune diseases, neurological diseases and transcriptional function (Fig. 4I). We verified the downregulated MMPs members in the sequencing results and found that PCGF1 could significantly down-regulate the expression of MMP8, MMP10, and MMP12 (Fig. 4J). Therefore, we speculate that PCGF1 regulates neuroinflammation by affecting the transcription of MMPs members.

PCGF1 regulates MMP10 expression through up-regulating RING1B/H2AK119ub and EZH2/H3K27me3

As PCGF1 is an epigenetic repressor and regulates gene transcription through histone modifications, the expression of related histone modifications was first measured. We found that PCGF1 could significantly upregulate the expression of H2AK119ub and H3K27me3 in primary microglia and BV2 microglia (Fig. 5A, B). After that, we used ChIP-QPCR to detect the binding of H2AK119ub and H3K27me3 in the MMPs promoter region in BV2 microglia. We found that only the binding of H2AK119ub and H3K27me3 in the MMP10 promoter region were affected by PCGF1 (Fig. 5C), while MMP8 (Fig. S5C) and MMP12 (Fig. S5D) were unchanged. As previously mentioned, the E3 ubiquitin ligase Ring1B in PRC1 primarily mediates H2AK119ub, and the methyltransferase EZH2 in PRC2 primarily mediates H3K27me3. Therefore, we examined the deposition of both enzymes in the MMP10 promoter region. ChIP-QPCR analysis demonstrated that the overexpression of PCGF1 led to an elevated deposition of PCGF1, RING1B and EZH2 (Fig. 5D–F) within the promoter region of MMP10. Immunoprecipitation results further revealed that PCGF1 directly binds to RING1B but not to EZH2 (Fig. 5G). As previously reported, H2AK119ub formed by PRC1 creates a binding site for PRC2 containing Jarid2-Aebp2 and promotes the deposition of H3K27me3 [56]. Thus, we propose that PCGF1 initially associates with RING1B and accumulates within the promoter region, concurrently promoting the deposition of H2AK119ub. Then, this cascade triggers the subsequent deposition of EZH2 and H3K27me3. Ultimately, their combined actions collectively suppress the transcriptional activity of the MMP10 promoter region.

Subsequently, we used ChIP-Seq to further investigate the relationship between PCGF1 and the MMP10 promoter. ChIP-Seq results showed that PCGF1 overexpression increased the binding peaks of PCGF1, H2AK119ub and H3K27me3 (Fig. 5H–J) in the promoter region of MMP10 (red box, 2000 bp), which is consistent with the results of ChIP-QPCR. The binding tracks of RING1B and EZH2 were detected by ChIP-QPCR (Fig. S5E–G). By Gene Ontology (GO) analysis of different PEAK-related genes after overexpression of PCGF1, we found that PCGF1 and H2AK119ub binding differential genes were enriched in the immune system, behavior, and transcriptional regulation (Fig. S5H, S5I). In addition, we performed Motif analysis of peak sequence and identified base characteristics of PCGF1/H2AK119ub/H3K27me3 binding (Fig. S5J).

PCGF1 regulates neuroinflammation possibly via the MMP10/NF-κB/MAPK pathways

After clarifying that PCGF1 can specifically regulate MMP10 transcription, we proceeded to verify the inhibitory effect of PCGF1 on MMP10. PCGF1 not only downregulated MMP10 mRNA expression in primary microglia (Fig. 4J) but also had the same inhibitory effect in CA1 region (Fig. S6A) and BV2 microglia

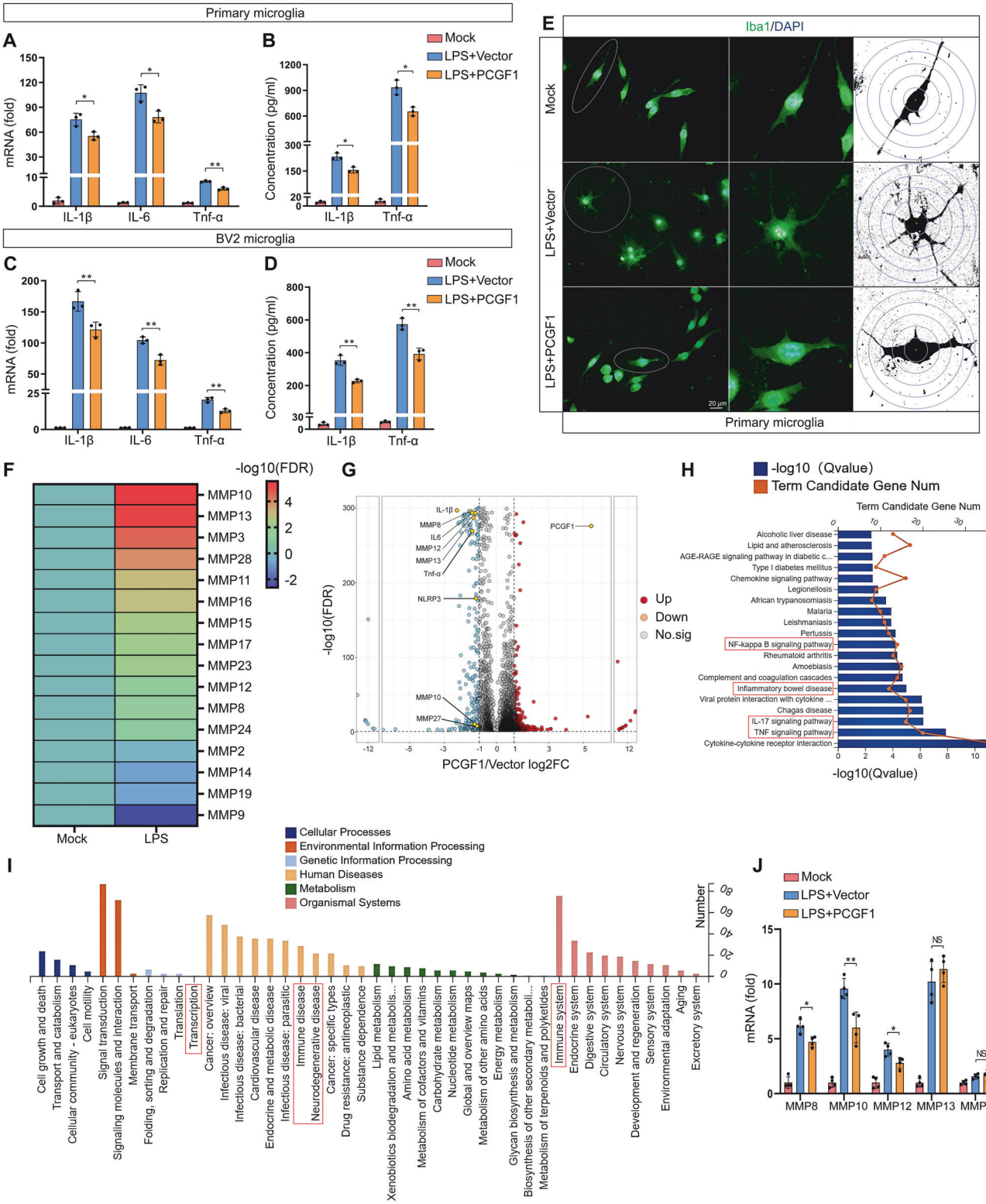

(Fig. S6B). Moreover, PCGF1 inhibited MMP10 expression at the protein levels (Fig. S6C, S6D). Immunofluorescence experiments in the CA1 region also demonstrated the above conclusions (Figs. 6A and S6E). Since the specific function of MMP10 in microglia has not been reported, we aimed to investigate how microglial MMP10 mediates neuroinflammation. Firstly, we knock down the MMP10 in primary microglia by lentivirus and assayed the knockdown efficiency (Fig. 6E). The results showed that knockdown of MMP10 decreased expression of IL-1β, IL-6, and Tnf-α at mRNA and protein levels (Fig. 6B, C). Here, we examined several signaling pathways associated with microglia activation, including NF-κB and MAPK. The results revealed that the LPS-induced p65

Fig. 4 Microglial PCGF1 regulates LPS-induced neuroinflammation by MMPs members. A, **B** QPCR analysis and ELISA analysis of IL-1β, IL-6 and Tnf-α levels in primary microglia ($N = 3$ per group). **C**, **D** QPCR analysis and ELISA analysis of IL-1β, IL-6 and Tnf-α levels in BV2 microglia ($N = 3$ per group). **E** Representative images of microglia morphology. Microglia (green) are stained with Iba1. Nuclei (blue) are stained with DAPI. Scale bar is 20 μm. **F** Expression heat map of MMPs members in primary microglia of Mock and LPS. **G** The volcano plot of differentially expressed genes in primary microglia transfected with PCGF1. **H** KEGG analysis revealed the differentially expressed genes were involved in inflammatory signaling pathways. **I** KEGG analysis revealed that the differentially expressed genes were enriched in immune diseases, neurological diseases and transcription function. **J** QPCR analysis of MMPs members mRNA levels in primary microglia transfected with PCGF1 ($N = 3$ per group). Statistical significance was determined by multiple unpaired two-sided Student's *t*-tests or one-way ANOVA followed by Tukey post hoc test. Data are shown as the mean±s.d. or as a representative result from three independent experiments. $^{*}P < 0.05$, $^{**}P < 0.01$ and $^{***}P < 0.001$.

entry into the nucleus was hindered (Fig. 6D) and the phosphorylation of p38, JNK, and p65 were inhibited (Fig. 6E, F) by MMP10 knockdown. Meanwhile, we used the phosphorylation inhibitors of p38 and p65, SB203580 and PDTC, to clarify that the NF-κB and MAPK pathways are also pro-inflammatory in primary microglia (Fig. S6F–I). The above results suggested that MMP10 is a pro-inflammatory factor and PCGF1 inhibits the expression of MMP10, which may prove to be an essential mechanism for PCGF1 in regulating neuroinflammation.

Then, we injected a mixture of PCGF1 and MMP10 overexpressed AAV9 virus in the CA1 region (Fig. S7A, S7B). We confirmed successful overexpression of PCGF1 and MMP10 in the CA1 region via western blotting (Fig. S7C). Successful virus targeting was indicated by the observation of large amounts of green (PCGF1-GFP) and red (MMP10-mcherry) fluorescence within the CA1 region (Fig. 6G). Subsequently, we found that MMP10 reversed the PCGF1-mediated remission of neuroinflammation (Fig. 6H). As previously shown, PCGF1 alleviated depression-like behavior caused by CUMS, while MMP10 reversed the function of PCGF1. MMP10 decreased sucrose solution consumption (Fig. 6I) and increased immobility time in FST (Fig. 6J) and TST (Fig. 6K). Meanwhile, MMP10 decreased the duration and frequency of mice exploring the central area in OFT (Fig. S7D–G). The results of EPM test also showed that MMP10 reduced the duration and frequency of mice entering the open arm (Fig. S7H–J). These results suggest that MMP10 of microglia may be the target of PCGF1 in regulating depression-like behavior.

DISCUSSION

Neuroinflammation generally refers to an inflammatory response within the CNS that can be induced by various pathological insults. This process is characterized by the expression of proinflammatory cytokines [57]. These cytokines can result in synaptic dysfunction, neuronal death, and impeded neurogenesis [58]. However, neuroinflammation tends to be a chronic process that cannot spontaneously resolve and is considered to be a major contributor to neuropsychiatric/neurodegenerative pathogenesis [59, 60]. The present research has provided the first evidence that PCGF1 in microglia is involved in regulating neuroinflammation associated with the pathological processes of adolescent depression. Specifically, PCGF1 potentially downregulates the MAPK/NF-kB pathway by targeting the downstream gene MMP10 to regulate neuroinflammation in the hippocampal CA1 region of mice. Furthermore, it helps to reduce depression-like behavior and neuronal damage in CUMS adolescent mice. These findings collectively suggest that PCGF1 functions as a crucial therapeutic target for regulating neuroinflammation during the pathogenesis of adolescent depression.

In the past decade, the prevalence of elevated depressive symptoms among adolescents has risen from 24% to 37% [61]. Nonetheless, significant etiological differences, including genetic structures and treatment responses, exist between adolescents and adults with depression. The efficacy of antidepressants in treating adolescent depression is not satisfactory [62]. In particular, selective serotonin reuptake inhibitors (SSRIs) and tricyclic antidepressants are less effective in the treatment of adolescent depression than in the treatment of adult depression [63, 64]. Therefore, it is crucial to explore alternative and more effective treatment options for adolescent depression. The adolescent period is recognized as a critically important phase of brain development [65], but the adult brain loses this unique plasticity [66]. Importantly, epigenetic mechanisms underpin these dynamic developmental processes [10, 11, 67], particularly during adolescence [68]. The dynamic epigenetic regulation of gene expression in response to environmental stimuli facilitates the acquisition of persistent molecular, cellular, and complex behavioral associations in organisms [66].

In our study, we found that the expression of PCGF1 decreased both in the plasma of adolescent MDD patients and in the microglia of adolescent mice in a mouse model of depression. As mentioned before, the role of the PCGF family in depression has not been reported. Research on PCGF1 has focused mainly on embryonic development [38–40], tumor stem cell self-renewal [30, 41, 42], and hematopoietic stem cell differentiation [43, 44]. However, for the first time, we demonstrated that PCGF1 also plays an essential role in regulating microglia-mediated neuroinflammation and ameliorates depression-like behavior in adolescent mice.

MMP-10, also known as stromelysin-2, is a zinc-dependent enzyme belonging to the ubiquitous matrix metalloproteinase superfamily [69]. MMPs are involved in physiological processes, such as tissue homeostasis, host defense, and tissue repair, by participating in the degradation of extracellular matrix proteins and the cleavage of cell adhesion molecules, cytokines, and growth factors [69, 70]. MMPs have emerged as novel biomarkers for depression, and MMP-9 has been reported to be significantly elevated in the plasma of patients with MDD [71]. Notably, functional studies of MMPs in microglia are becoming a new research hotspot but have focused primarily on MMP3 [72], MMP8 [73], and MMP9 [74], with less attention directed toward MMP10. Cerebrospinal fluid levels of MMP-10 reflect aging and neuroinflammation and can be used as a prognostic marker for Alzheimer's disease [75]. In our study, we found that in microglia, MMP10 exerts a proinflammatory effect by regulating the entry of P65 into the nucleus and the phosphorylation of NF-κB and the MAPK pathway.

In summary, our study revealed a novel mechanism for treating adolescent depression by linking neuroinflammation to epigenetics. Specifically, we found that microglial PCGF1 inhibits NF-κB/MAPK pathway activation through the regulation of RING1B/H2AK119ub and EZH2/H3K27me3 in the MMP10 promoter region. Notably, although using LPS for in vitro experiments to induce neuroinflammation is a well-established way to mimic neuroinflammation in vivo, the effects of LPS are not fully consistent with those of CUMS. Furthermore, the results showed that the effect of PCGF1 overexpression in vivo seems to be stronger compared to the in vitro experiments. The possible reason is that the brain is a complex system, when homeostasis is disrupted in the brain,

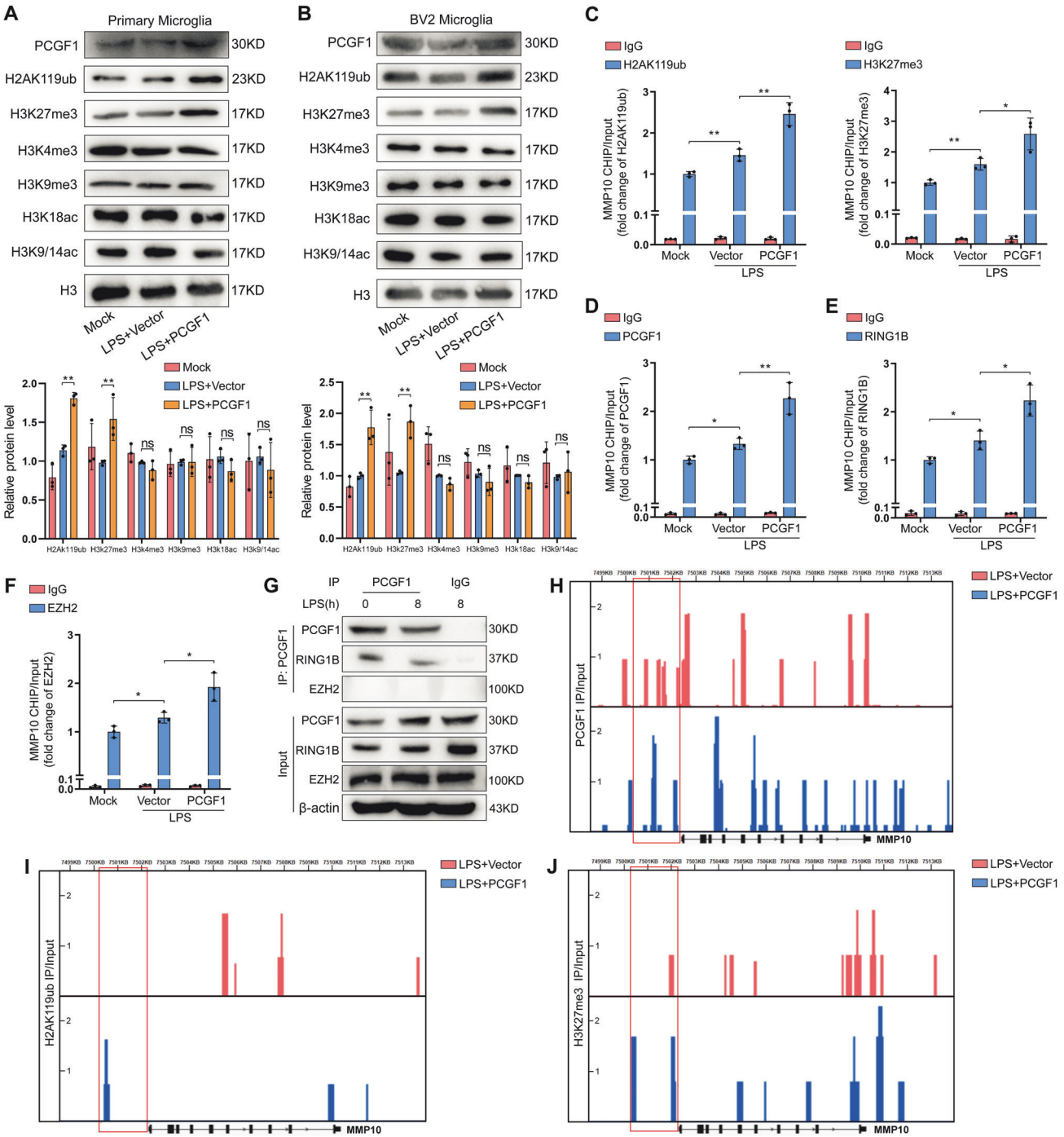

Fig. 5 PCGF1 regulates histone modification in the MMP10 promoter region. A, **B** Representative western blot images showing the expression of relative histone modifications in primary microglia or BV2 microglia ($N = 3$ per group). **C** ChIP-QPCR analysis identified the expression of H2AK119ub and H3K27me3 at the promoters of MMP10 in BV2 microglia. **D**–**F** ChIP-QPCR analysis identified the expression of PCGF1, RING1B and EZH2 at the promoters of MMP10 in BV2 microglia ($N = 3$ per group). **G** Immunoprecipitation (IP) demonstrating that PCGF1 binds to RING1B but not to EZH2 in BV2 microglia. **H**–**J** The binding peaks of PCGF1, H2AK119ub and H3K27me3 in the MMP10 promoter region from ChIP-seq. Statistical significance was determined by multiple unpaired two-sided Student's *t*-tests or one-way ANOVA followed by Tukey post hoc test. Data are shown as the mean±s.d. or as a representative result from three independent experiments. $^{*}P < 0.05$, $^{**}P < 0.01$ and $^{***}P < 0.001$.

all types of immune cells are activated, generating an inflammatory cascade and releasing more inflammatory factors. Our data strongly support these hypothesized mechanisms, additional studies are needed to confirm our findings. In conclusion, our study reveals a new target molecule and sheds light on some mechanisms involved in the onset of adolescent depression, providing promising therapeutic options for treating this disorder.

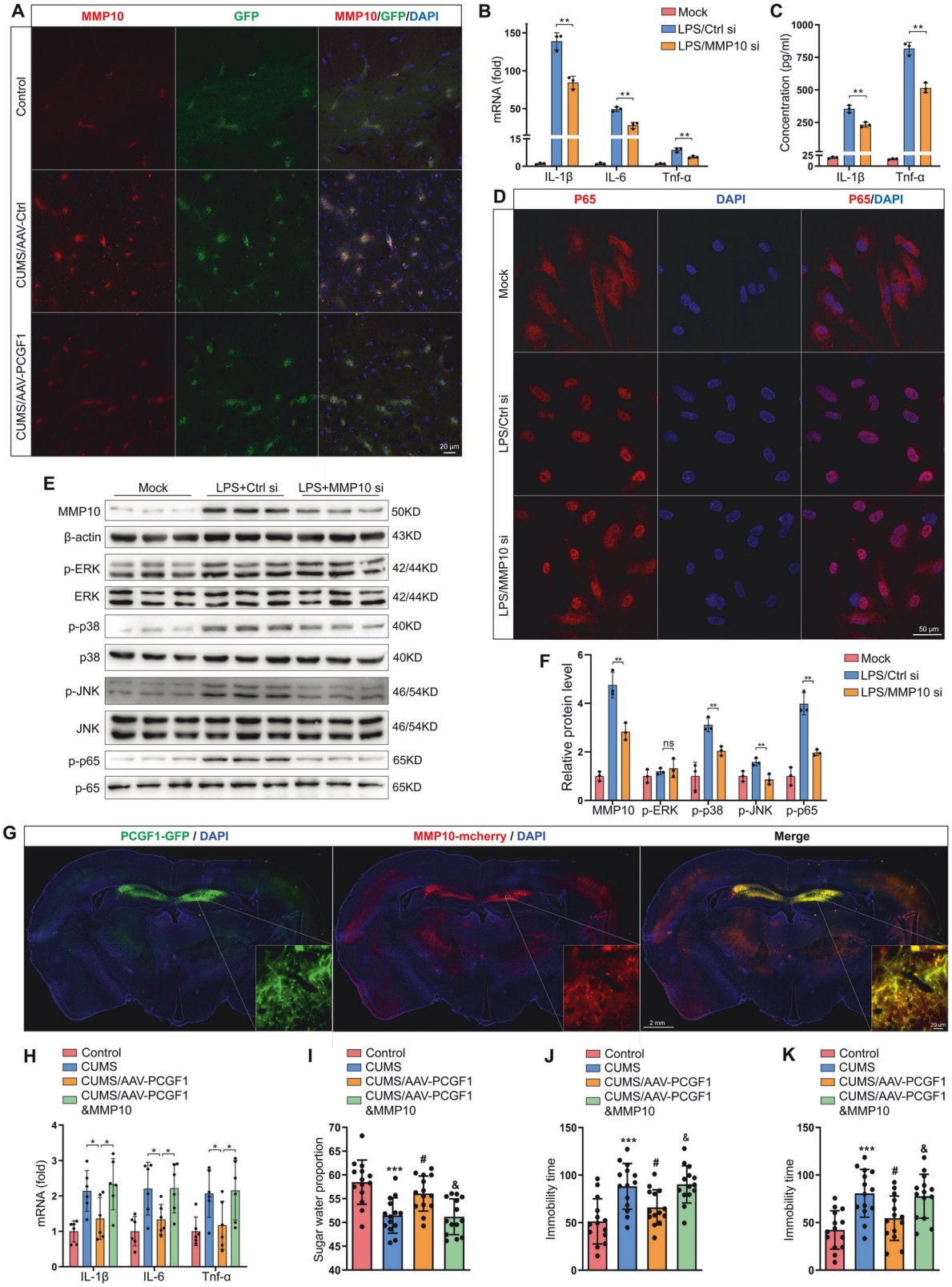
A
MMP10
GFP
MMP10/GFP/DAPI
Control
CUMS/AAV-Ctrl
CUMS/AAV-PCGF1
20 μm
B
Mock
LPS/Ctrl si
LPS/MMP10 si
mRNA (fold)
IL-1β
IL-6
Tnf-α
C
Concentration (pg/ml)
IL-1β
Tnf-α
D
P65
DAPI
P65/DAPI
Mock
LPS/Ctrl si
LPS/MMP10 si
50 μm
E
Mock
LPS+Ctrl si
LPS+MMP10 si
MMP10
β-actin
p-ERK
ERK
p-p38
p38
p-JNK
JNK
p-p65
p-65
50KD
43KD
42/44KD
42/44KD
40KD
40KD
46/54KD
46/54KD
65KD
65KD
F
Relative protein level
Mock
LPS/Ctrl si
LPS/MMP10 si
MMP10
p-ERK
p-p38
p-JNK
p-p65
ns
G
PCGF1-GFP / DAPI
MMP10-mcherry / DAPI
Merge
2 mm
20 μm
H
Control
CUMS
CUMS/AAV-PCGF1
CUMS/AAV-PCGF1 &MMP10
mRNA (fold)
IL-1β
IL-6
Tnf-α
I
Control
CUMS
CUMS/AAV-PCGF1
CUMS/AAV-PCGF1 &MMP10
Sugar water proportion
J
Control
CUMS
CUMS/AAV-PCGF1
CUMS/AAV-PCGF1 &MMP10
Immobility time
K
Control
CUMS
CUMS/AAV-PCGF1
CUMS/AAV-PCGF1 &MMP10
Immobility time

Fig. 6 PCGF1 inhibits neuroinflammation via the MMP10/NF-κB/MAPK pathway. A Representative image of MMP10 (red) and GFP (green). Nuclei (blue) are stained with DAPI. Scale bar is 20 μm. **B** QPCR analysis of IL-1β, IL-6 and Tnf-α mRNA levels in primary microglia ($N = 3$ per group). **C** ELISA analysis of IL-1β and Tnf-α secretion in primary microglia ($N = 3$ per group). **D** Representative images of p65 (red) enters the nucleus. Nuclei (blue) are stained with DAPI. Scale bar is 50 μm. **E**, **F** Representative western blot images showing the expression of MMP10 and the phosphorylation of ERK, p38, JNK and p65 ($N = 3$ per group). **G** Schematics of AAV vectors and bilateral injection sites in the CA1 region of hippocampus. Scale bar, 2 mm and 20 μm. **H** QPCR analysis of IL-1β, IL-6 and Tnf-α mRNA levels of CA1 region ($N = 6$ per group). **I** MMP10 reduced sucrose solution consumption ($N = 14$ per group, * CUMS vs. Control; # CUMS/AAV-PCGF1 vs. CUMS; & CUMS/AAV-PCGF1/MMP10 vs. CUMS/AAV-PCGF1; the same below). **J**, **K** MMP10 increased immobility time in FST and TST ($N = 14$ per group). Statistical significance was determined by multiple unpaired two-sided Student's *t*-tests or one-way ANOVA followed by Tukey post hoc test. Data are shown as the mean±s.d. or as a representative result from three independent experiments. $^*P < 0.05$, $^{**}P < 0.01$ and $^{***}P < 0.001$. # and & follows the same rules.

DATA AVAILABILITY

All data needed to evaluate the conclusions in the paper are present in the paper and/or the Supplementary Materials. We uploaded the raw data of sequencing to National Center for Biotechnology Information (NCBI) DataBase with BioProject ID PRJNA1148989.

REFERENCES

1. Malhi GS, Mann JJ. Depression. Lancet. 2018;392:2299–312.
2. Collaborators GBDMD. Global, regional, and national burden of 12 mental disorders in 204 countries and territories, 1990-2019: a systematic analysis for the Global Burden of Disease Study 2019. Lancet Psychiatry. 2022;9:137–50.
3. Malhi GS, Outhred T, Hamilton A, Boyce PM, Bryant R, Fitzgerald PB, et al. Royal Australian and New Zealand College of Psychiatrists clinical practice guidelines for mood disorders: major depression summary. Med J Aust. 2018;208:175–80.
4. Patton GC, Sawyer SM, Santelli JS, Ross DA, Afifi R, Allen NB, et al. Our future: a Lancet commission on adolescent health and wellbeing. Lancet. 2016;387:2423–78.
5. Diener MJ, Gottdiener WH, Keefe JR, Levy KN, Midgley N. Treatment of depression in children and adolescents. Lancet Psychiatry. 2021;8:97.
6. Collishaw S. Annual research review: secular trends in child and adolescent mental health. J Child Psychol Psychiatry. 2015;56:370–93.
7. Mychasiuk R, Metz GA. Epigenetic and gene expression changes in the adolescent brain: what have we learned from animal models? Neurosci Biobehav Rev. 2016;70:189–97.
8. Luciana M. Adolescent brain development in normality and psychopathology. Dev Psychopathol. 2013;25:1325–45.
9. Li M, Santpere G, Imamura Kawasawa Y, Evgrafov OV, Gulden FO, Pochareddy S, et al. Integrative functional genomic analysis of human brain development and neuropsychiatric risks. Science. 2018;362:eaat7615.
10. Paus T, Keshavan M, Giedd JN. Why do many psychiatric disorders emerge during adolescence? Nat Rev Neurosci. 2008;9:947–57.
11. McCarroll SA, Hyman SE. Progress in the genetics of polygenic brain disorders: significant new challenges for neurobiology. Neuron. 2013;80:578–87.
12. Bae BI, Jayaraman D, Walsh CA. Genetic changes shaping the human brain. Dev Cell. 2015;32:423–34.
13. Dalton VS, Kolshus E, McLoughlin DM. Epigenetics and depression: return of the repressed. J Affect Disord. 2014;155:1–12.
14. Hwang JY, Aromolaran KA, Zukin RS. The emerging field of epigenetics in neurodegeneration and neuroprotection. Nat Rev Neurosci. 2017;18:347–61.
15. Bagert JD, Muir TW. Molecular epigenetics: chemical biology tools come of age. Annu Rev Biochem. 2021;90:287–320.
16. Roy B, Wang Q, Palkovits M, Faludi G, Dwivedi Y. Altered miRNA expression network in locus coeruleus of depressed suicide subjects. Sci Rep. 2017;7:4387.
17. Yoshino Y, Dwivedi Y. Non-coding RNAs in psychiatric disorders and suicidal behavior. Front Psychiatry. 2020;11:543893.
18. Roy B, Shelton RC, Dwivedi Y. DNA methylation and expression of stress related genes in PBMC of MDD patients with and without serious suicidal ideation. J Psychiatr Res. 2017;89:115–24.
19. Wu YL, Lin ZJ, Li CC, Lin X, Shan SK, Guo B, et al. Epigenetic regulation in metabolic diseases: mechanisms and advances in clinical study. Signal Transduct Target Ther. 2023;8:98.
20. Wolffe AP, Hayes JJ. Chromatin disruption and modification. Nucleic Acids Res. 1999;27:711–20.
21. Hansen JC, Tse C, Wolffe AP. Structure and function of the core histone N-termini: more than meets the eye. Biochemistry. 1998;37:17637–41.
22. Strahl BD, Allis CD. The language of covalent histone modifications. Nature. 2000;403:41–45.
23. Luo Y, Fang Y, Kang R, Lenahan C, Gamdzyk M, Zhang Z, et al. Inhibition of EZH2 (enhancer of Zeste Homolog 2) attenuates neuroinflammation via H3k27me3/SOCS3/TRAF6/NF-kappaB (trimethylation of histone 3 lysine 27/suppressor of cytokine signaling 3/tumor necrosis factor receptor family 6/nuclear factor-kappaB) in a rat model of subarachnoid hemorrhage. Stroke. 2020;51:3320–31.
24. Rigillo G, Vilella A, Benatti C, Schaeffer L, Brunello N, Blom JMC, et al. LPS-induced histone H3 phospho(Ser10)-acetylation(Lys14) regulates neuronal and microglial neuroinflammatory response. Brain Behav Immun. 2018;74:277–90.
25. Zheng SZ, Zhang XW, Song XM, Yang Z, Yao L, Tu PF, et al. Epoxymicheliolide directly targets histone H2B to inhibit neuroinflammation via recruiting E3 ligase RNF20. Pharmacol Res. 2022;177:106093.
26. Singh G, Singh V, Schneider JS. Post-translational histone modifications and their interaction with sex influence normal brain development and elaboration of neuropsychiatric disorders. Biochim Biophys Acta Mol Basis Dis. 2019;1865:1968–81.
27. Zhao X, Ueba T, Christie BR, Barkho B, McConnell MJ, Nakashima K, et al. Mice lacking methyl-CpG binding protein 1 have deficits in adult neurogenesis and hippocampal function. Proc Natl Acad Sci USA. 2003;100:6777–82.
28. Liu Y, Li M, Fan M, Song Y, Yu H, Zhi X, et al. Chromodomain Y-like protein-mediated histone crotonylation regulates stress-induced depressive behaviors. Biol Psychiatry. 2019;85:635–49.
29. Gundersen BB, Blendy JA. Effects of the histone deacetylase inhibitor sodium butyrate in models of depression and anxiety. Neuropharmacology. 2009;57:67–74.
30. Gong Y, Yue J, Wu X, Wang X, Wen J, Lu L, et al. NSPc1 is a cell growth regulator that acts as a transcriptional repressor of p21Waf1/Cip1 via the RARE element. Nucleic Acids Res. 2006;34:6158–69.
31. Blackledge NP, Rose NR, Klose RJ. Targeting polycomb systems to regulate gene expression: modifications to a complex story. Nat Rev Mol Cell Biol. 2015;16:643–9.
32. Farcas AM, Blackledge NP, Sudbery I, Long HK, McGouran JF, Rose NR, et al. KDM2B links the polycomb repressive complex 1 (PRC1) to recognition of CpG islands. eLife. 2012;1:e00205.
33. Blackledge NP, Fursova NA, Kelley JR, Huseyin MK, Feldmann A, Klose RJ. PRC1 catalytic activity is central to polycomb system function. Mol Cell. 2020;77:857–74 e859.
34. Laugesen A, Hojfeldt JW, Helin K. Molecular mechanisms directing PRC2 recruitment and H3K27 methylation. Mol Cell. 2019;74:8–18.
35. Yu JR, Lee CH, Oksuz O, Stafford JM, Reinberg D. PRC2 is high maintenance. Genes Dev. 2019;33:903–35.
36. Blackledge NP, Farcas AM, Kondo T, King HW, McGouran JF, Hanssen LLP, et al. Variant PRC1 complex-dependent H2A ubiquitylation drives PRC2 recruitment and polycomb domain formation. Cell. 2014;157:1445–59.
37. Sugishita H, Kondo T, Ito S, Nakayama M, Yakushiji-Kaminatsui N, Kawakami E, et al. Variant PCGF1-PRC1 links PRC2 recruitment with differentiation-associated transcriptional inactivation at target genes. Nat Commun. 2021;12:5341.
38. Zhu Y, Dong L, Wang C, Hao K, Wang J, Zhao L, et al. Functional redundancy among Polycomb complexes in maintaining the pluripotent state of embryonic stem cells. Stem Cell Rep. 2022;17:1198–214.
39. Li X, Ji G, Zhou J, Du J, Li X, Shi W, et al. Pcgf1 regulates early neural tube development through histone methylation in Zebrafish. Front Cell Dev Biol. 2020;8:581636.
40. Yan Y, Zhao W, Huang Y, Tong H, Xia Y, Jiang Q, et al. Loss of polycomb group protein Pcgf1 severely compromises proper differentiation of embryonic stem cells. Sci Rep. 2017;7:46276.
41. Hu PS, Xia QS, Wu F, Li DK, Qi YJ, Hu Y, et al. NSPc1 promotes cancer stem cell self-renewal by repressing the synthesis of all-trans retinoic acid via targeting RDH16 in malignant glioma. Oncogene. 2017;36:4706–18.
42. Ji G, Zhou W, Du J, Zhou J, Wu D, Zhao M, et al. PCGF1 promotes epigenetic activation of stemness markers and colorectal cancer stem cell enrichment. Cell Death Dis. 2021;12:633.
43. Ross K, Sedello AK, Todd GP, Paszkowski-Rogacz M, Bird AW, Ding L, et al. Polycomb group ring finger 1 cooperates with Runx1 in regulating differentiation and self-renewal of hematopoietic cells. Blood. 2012;119:4152–61.

44. Takano J, Ito S, Dong Y, Sharif J, Nakajima-Takagi Y, Umeyama T, et al. PCGF1-PRC1 links chromatin repression with DNA replication during hematopoietic cell lineage commitment. Nat Commun. 2022;13:7159.
45. Bie B, Wu J, Yang H, Xu JJ, Brown DL, Naguib M. Epigenetic suppression of neuroligin 1 underlies amyloid-induced memory deficiency. Nat Neurosci. 2014;17:223–31.
46. Nikolopoulos D, Manolakou T, Polissidis A, Filia A, Bertsias G, Koutmani Y, et al. Microglia activation in the presence of intact blood-brain barrier and disruption of hippocampal neurogenesis via IL-6 and IL-18 mediate early diffuse neuropsychiatric lupus. Ann Rheum Dis. 2023;82:646–57.
47. Setiawan E, Wilson AA, Mizrahi R, Rusjan PM, Miler L, Rajkowska G, et al. Role of translocator protein density, a marker of neuroinflammation, in the brain during major depressive episodes. JAMA Psychiatry. 2015;72:268–75.
48. Miller AH, Maletic V, Raison CL. Inflammation and its discontents: the role of cytokines in the pathophysiology of major depression. Biol Psychiatry. 2009;65:732–41.
49. Shelton RC, Claiborne J, Sidoryk-Wegrzynowicz M, Reddy R, Aschner M, Lewis DA, et al. Altered expression of genes involved in inflammation and apoptosis in frontal cortex in major depression. Mol Psychiatry. 2011;16:751–62.
50. Hare BD, Duman RS. Prefrontal cortex circuits in depression and anxiety: contribution of discrete neuronal populations and target regions. Mol Psychiatry. 2020;25:2742–58.
51. Ferri J, Ford JM, Roach BJ, Turner JA, van Erp TG, Voyvodic J, et al. Resting-state thalamic dysconnectivity in schizophrenia and relationships with symptoms. Psychol Med. 2018;48:2492–9.
52. Wu Y, Zheng Y, Li J, Liu Y, Liang X, Chen Y, et al. Subregion-specific, modality-dependent and timescale-sensitive hippocampal connectivity alterations in patients with first-episode, drug-naive major depression disorder. J Affect Disord. 2022;305:159–72.
53. Lin PY, Ma ZZ, Mahgoub M, Kavalali ET, Monteggia LM. A synaptic locus for TrkB signaling underlying ketamine rapid antidepressant action. Cell Rep. 2021;36:109513.
54. Yuan M, Rubin-Falcone H, Lin X, Rizk MM, Miller JM, Sublette ME, et al. Smaller left hippocampal subfield CA1 volume is associated with reported childhood physical and/or sexual abuse in major depression: a pilot study. J Affect Disord. 2020;272:348–54.
55. Magee JC, Grienberger C. Synaptic plasticity forms and functions. Annu Rev Neurosci. 2020;43:95–117.
56. Kalb R, Latwiel S, Baymaz HI, Jansen PW, Muller CW, Vermeulen M, et al. Histone H2A monoubiquitination promotes histone H3 methylation in Polycomb repression. Nat Struct Mol Biol. 2014;21:569–71.
57. DiSabato DJ, Quan N, Godbout JP. Neuroinflammation: the devil is in the details. J Neurochem. 2016;139:136–53.
58. Lyman M, Lloyd DG, Ji X, Vizcaychipi MP, Ma D. Neuroinflammation: the role and consequences. Neurosci Res. 2014;79:1–12.
59. Heneka MT, Carson MJ, El Khoury J, Landreth GE, Brosseron F, Feinstein DL, et al. Neuroinflammation in Alzheimer's disease. Lancet Neurol. 2015;14:388–405.
60. Li B, Yang W, Ge T, Wang Y, Cui R. Stress induced microglial activation contributes to depression. Pharmacol Res. 2022;179:106145.
61. Shorey S, Ng ED, Wong CHJ. Global prevalence of depression and elevated depressive symptoms among adolescents: A systematic review and meta-analysis. Br J Clin Psychol. 2022;61:287–305.
62. Cipriani A, Zhou X, Del Giovane C, Hetrick SE, Qin B, Whittington C, et al. Comparative efficacy and tolerability of antidepressants for major depressive disorder in children and adolescents: a network meta-analysis. Lancet. 2016;388:881–90.
63. Jane Garland E, Kutcher S, Virani A, Elbe D. Update on the use of SSRIs and SNRIs with children and adolescents in clinical practice. J Can Acad Child Adolesc Psychiatry. 2016;25:4–10.
64. Hazell P, O'Connell D, Heathcote D, Robertson J, Henry D. Efficacy of tricyclic drugs in treating child and adolescent depression: a meta-analysis. BMJ. 1995;310:897–901.
65. Tau GZ, Peterson BS. Normal development of brain circuits. Neuropsychopharmacology. 2010;35:147–68.
66. Fagiolini M, Jensen CL, Champagne FA. Epigenetic influences on brain development and plasticity. Curr Opin Neurobiol. 2009;19:207–12.
67. Keshavan MS, Giedd J, Lau JY, Lewis DA, Paus T. Changes in the adolescent brain and the pathophysiology of psychotic disorders. Lancet Psychiatry. 2014;1:549–58.
68. Somel M, Franz H, Yan Z, Lorenc A, Guo S, Giger T, et al. Transcriptional neoteny in the human brain. Proc Natl Acad Sci USA. 2009;106:5743–8.
69. Sternlicht MD, Werb Z. How matrix metalloproteinases regulate cell behavior. Annu Rev Cell Dev Biol. 2001;17:463–516.
70. Parks WC, Wilson CL, Lopez-Boado YS. Matrix metalloproteinases as modulators of inflammation and innate immunity. Nat Rev Immunol. 2004;4:617–29.
71. Domenici E, Wille DR, Tozzi F, Prokopenko I, Miller S, McKeown A, et al. Plasma protein biomarkers for depression and schizophrenia by multi analyte profiling of case-control collections. PLoS ONE. 2010;5:e9166.
72. Lee JY, Choi HY, Yune TY. MMP-3 secreted from endothelial cells of blood vessels after spinal cord injury activates microglia, leading to oligodendrocyte cell death. Neurobiol Dis. 2015;82:141–51.
73. Lee EJ, Han JE, Woo MS, Shin JA, Park EM, Kang JL, et al. Matrix metalloproteinase-8 plays a pivotal role in neuroinflammation by modulating TNF-alpha activation. J Immunol. 2014;193:2384–93.
74. Hannocks MJ, Zhang X, Gerwien H, Chashchina A, Burmeister M, Korpos E, et al. The gelatinases, MMP-2 and MMP-9, as fine tuners of neuroinflammatory processes. Matrix Biol. 2019;75-76:102–13.
75. Martino Adami PV, Orellana A, Garcia P, Kleineidam L, Alarcon-Martin E, Montrreal L, et al. Matrix metalloproteinase 10 is linked to the risk of progression to dementia of the Alzheimer's type. Brain. 2022;145:2507–17.

ACKNOWLEDGEMENTS

We thank the Translational Medicine Core Facility of Shandong University for instrumental support.

AUTHOR CONTRIBUTIONS

Conceptualization: AH, WZ, NL. Performed experiments: NL. Data collection and analysis: NL, JD, YY, TZ. Investigation: NL, DW, PF, DSW. Funding acquisition: AH, WZ, LK. Writing—original draft: NL. Writing—review & editing: AH, WZ, LK. Supervision: AH.

FUNDING

This study was supported by funding from the National Natural Science Foundation of China (No. 81771219, 82071267 and 82001214), Foundation of Jinan (No. 2021GXRC103) and the Special Foundation for Taishan Scholars (No. tsqn202211034).

COMPETING INTERESTS

The authors declare no competing interests.

ADDITIONAL INFORMATION

Supplementary information The online version contains supplementary material available at https://doi.org/10.1038/s41380-024-02714-2.

Correspondence and requests for materials should be addressed to Linghua Kong, Wenjuan Zhou or Aijun Hao.

Reprints and permission information is available at http://www.nature.com/reprints

Publisher's note Springer Nature remains neutral with regard to jurisdictional claims in published maps and institutional affiliations.

Open Access This article is licensed under a Creative Commons Attribution-NonCommercial-NoDerivatives 4.0 International License, which permits any non-commercial use, sharing, distribution and reproduction in any medium or format, as long as you give appropriate credit to the original author(s) and the source, provide a link to the Creative Commons licence, and indicate if you modified the licensed material. You do not have permission under this licence to share adapted material derived from this article or parts of it. The images or other third party material in this article are included in the article's Creative Commons licence, unless indicated otherwise in a credit line to the material. If material is not included in the article's Creative Commons licence and your intended use is not permitted by statutory regulation or exceeds the permitted use, you will need to obtain permission directly from the copyright holder. To view a copy of this licence, visit http://creativecommons.org/licenses/by-nc-nd/4.0/.

© The Author(s) 2024